

# Inhibitive Properties, Thermodynamic and Quantum Chemical Studies of Azole Derivatives on Mild Steel Corrosion in $H_3PO_4$ Solutions

A.M.El-desoky<sup>\*1</sup>, Hala.M.Hassan<sup>2</sup>, Awad Al-Rashdi<sup>3</sup> and Marwa R. Elsayad<sup>4</sup>

<sup>\*1</sup>Engineering Chemistry Department, High Institute of Engineering & Technology (New Damietta), Egypt and Al-Qunfudah Center for Scientific Research (QCSR), Al-Qunfudah University College, Umm Al-Qura University, KSA.

<sup>2</sup>Textile Technology Department, Industrial Education College, Beni-Suef University, Egypt and Chemistry Department, Faculty of Science, Jazan University, KSA.

<sup>3</sup>Al-Qunfudah Center for Scientific Research (QCSR), Chemistry Department, Al-Qunfudah University College, Umm Al-Qura University, KSA.

<sup>4</sup>Ophthalmology Dept., Faculty of Medicine, Mansoura University, Egypt and Al-Qunfudah Center for Scientific Research (QCSR), Al-Qunfudah University College, Umm Al-Qura University, KSA.

**Abstract**—The inhibition of the corrosion of mild steel in 1 M  $H_3PO_4$  solutions by some azole derivatives has been investigated using weight loss, potentiodynamic polarization, electrochemical impedance spectroscopy (EIS) and electrochemical frequency modulation (EFM) techniques. Inhibition was found to increase with increasing concentration of the azole derivatives but decreased with rise in temperature. The inhibition was assumed to occur via adsorption of the inhibitor molecules on the metal surface. The adsorption of these compounds on mild steel surface obeys the Temkin's adsorption isotherm. Potentiodynamic polarization measurements showed that azole derivatives act as mixed-type inhibitors. Further, theoretical calculations were carried out and relations between computed parameters and experimental inhibition efficiency were discussed.

**Keywords**- Mild steel; Corrosion Inhibition; Azole Derivatives; Phosphoric Acid; Quantum Chemical Calculations.

## 1 INTRODUCTION

Phosphoric acid ( $H_3PO_4$ ) is a medium-strong acid, but it still shows strong corrosiveness on ferrous alloy [1].

$H_3PO_4$  is widely used in surface treatment of steel such as chemical and electrolytic polishing, chemical coloring, chemical and electrolytic etching, removal of oxide film, phosphating, passivating, and surface cleaning. Little work appears to have been done on the inhibition of mild steel in  $H_3PO_4$  solution. Using inhibitors is an effective method for corrosion to control the corrosion of metals. Inhibitors are compounds that control corrosion processes of metals. Many studies on inhibitors have been carried out [2-24], among them nitrogen containing inhibitor is one of the focuses of the studies [8-24]. Bentiss et al. [11], El Azhar et al. [16] and Elkadi et al. [20] have investigated many nitrogen-containing inhibitors for the corrosion inhibition of mild steel in HCl and  $H_2SO_4$ , their studies show that nitrogen-containing organic inhibitor acts as a strong inhibitor for mild steel in HCl, compared with  $H_2SO_4$ . Triazole and triazole-type compounds containing nitrogen, sulphur and heterocycle on the corrosion inhibition of metal in acidic media have attracted more attention because of their excellent corrosion inhibition performance [25-28]. The researches by Fouda et al. showed that some 4-phenylthiazole derivatives could inhibit the corrosion of 304L stainless steel in hydrochloric acid solution, but the inhibition effect was not very excellent [29]. However, synergistic effect occurred on addition of KSCN to acid containing 4-phenylthiazole derivatives which inhibited 304L stainless steel corrosion, and the phenomenon of synergism took place at very low concentrations for the systems studied. Wang et al. also investigated the

effect of some mercapto-triazole derivatives synthesized containing different hetero atoms and substituents in the organic structures on the corrosion and hydrogen permeation of mild steel in hydrochloric acid solution and their results revealed that all the mercapto-triazole derivatives performed excellently as corrosion inhibitors [30]. Especially, some N- and S-containing triazole derivatives are environmentally friendly corrosion inhibitors compared with some commercial acid corrosion inhibitors which are highly toxic, such as chromate and nitrite [31]. Little work appears to have been done on the inhibition of mild steel in  $H_3PO_4$  solution.

The aim of this work is to determine some thermodynamic activation Parameters Characterizing the Adsorption and Inhibitive Properties of some azole derivatives on mild steel corrosion in  $H_3PO_4$  Solutions. Also, to examine the relationship between quantum chemical calculations and experimental protection efficiencies of the tested azole derivatives by determining various quantum chemical parameters, these parameters include the highest occupied molecular orbital ( $E_{HOMO}$ ) and the lowest unoccupied molecular orbital ( $E_{LUMO}$ ), the energy difference ( $\Delta E$ ) between  $E_{HOMO}$  and  $E_{LUMO}$ .

## 2. Experimental Methods

### 2.1. Materials

Materials used for the study were mild steel sheet of composition (wt%) 0.20 C, 0.029 Si, 0.018 S, 0.0067 P, 0.397 Mn, 0.025 Ni, 0.0076 Cr, 0.0020 Mo, 0.0010 V, 0.036 Cu, 0.0010 Sn,

0.0057 Co, 0.126 Al, 0.023 Zn, 0.0020 Mg, 0.0046 Nb, and 0.0025 Bi, the rest Fe.

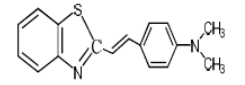
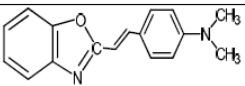
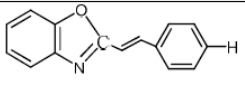
## 2.2. CHEMICALS AND SOLUTIONS

### 2.2.1. CHEMICALS

- Phosphoric acid (H<sub>3</sub>PO<sub>4</sub>) (BDH grade) and  
b- Organic additives

The organic inhibitors used in this study were listed in Table (1) [32].

TABLE 1  
Molecular Structures of Some Azole Derivatives

Cpd.	Structure	Name	Chemical Formula Molecular Weight
(1)		(E)-4-(2-(benzo[d]thiazol-2-yl)vinyl)-N,N-dimethylaniline	C <sub>17</sub> H <sub>16</sub> N <sub>2</sub> S 280.39
(2)		(E)-4-(2-(benzo[d]oxazol-2-yl)vinyl)-N,N-dimethylaniline	C <sub>17</sub> H <sub>16</sub> N <sub>2</sub> O 264.32
(3)		(E)-2-styrylbenzo[d]oxazole	C <sub>15</sub> H <sub>11</sub> NO 221.25

### 2.3. Weight Loss Method

Mild steel sheets of 20 mm x 20 mm x 2 mm were abraded with different grades of emery paper up to 1200 grit and then washed with bidistilled water and acetone. After weighing accurately, the specimens were immersed in 100 ml H<sub>3</sub>PO<sub>4</sub> solution with and without addition of different concentrations of inhibitors. After three hrs, the specimens were taken out, washed, dried, and weighed accurately. The average weight loss of the three parallel mild steel sheets could be obtained at required temperature. The inhibition efficiency (% IE) and the degree of surface coverage ( $\theta$ ) of the investigated inhibitors on the corrosion of mild steel were calculated as follows [33]:

$$\% \text{ IE} = [(W_0 - W) / W_0] \times 100 \quad (1)$$

$$\theta = \frac{W_0 - W}{W_0} \quad (2)$$

Where  $W_0$  and  $W$  are the values of the average weight loss in the absence and presence of the inhibitor, respectively.

### 2.4. Electrochemical Measurements

The experiments were carried out potentiodynamically in a thermostated three electrode cell. Platinum foil was used as counter electrode and a saturated calomel electrode (SCE) coupled to a fine Luggin capillary as the reference electrode. The working electrode was in the form of a square cut from mild steel under investigation and was embedded in a Teflon rod with an exposed area of 1 cm<sup>2</sup>. This electrode was immersed in 100 ml of a test solution for 30 min until a steady

state open-circuit potential ( $E_{ocp}$ ) was attained. Potentiodynamic polarization was conducted in an electrochemical system (Gamry framework instruments version 3.20) which comprises a PCI/ 300 potentiostat, controlled by a computer recorded and stored the data. The potentiodynamic curves were recorded by changing the electrode potential from -1.0 to 0.0 V versus SCE with scan rate of 5 mV/s. All experiments were carried out in freshly prepared solution at constant temperature (25 ± 1 °C) using a thermostat. IE% and the degree of surface coverage ( $\theta$ ) were defined as:

$$\% \text{ IE} = \frac{(i_{corr} - i_{corr(inh)})}{i_{corr}} \times 100 \quad (3)$$

$$\theta = \frac{(i_{corr} - i_{corr(inh)})}{i_{corr}} \quad (4)$$

Where  $i_{corr}$  and  $i_{corr(inh)}$  are the uninhibited and inhibited corrosion current density values, respectively, determined by extrapolation of Tafel lines.

The electrochemical impedance spectroscopy (EIS) spectra were recorded at open circuit potential (OCP) after immersion the electrode for 15 min in the test solution. The ac signal was 5 mV peak to peak and the frequency range studied was between 100 kHz and 0.2 Hz. All Electrochemical impedance experiments were carried out using Potentiostat/Galvanostat/Zra analyzer (Gamry PCI 300/4). A personal computer with EIS300 software and Echem Analyst 5.21 was used for data fitting and calculating.

The inhibition efficiency (% IE) and the surface coverage ( $\theta$ ) of the used inhibitors obtained from the impedance measurements were calculated by applying the following relations:

$$\text{IE}\% = \left( 1 - \frac{R_{ct}^0}{R_{ct}} \right) \times 100\% \quad (5)$$

$$\theta = \left( 1 - \frac{R_{ct}^0}{R_{ct}} \right) \quad (6)$$

Where,  $R_{ct}^0$  and  $R_{ct}$  are the charge transfer resistance in the absence and presence of inhibitor, respectively.

## 2.5 THEORETICAL STUDY

Accelrys (Material Studio Version 4.4) software for quantum chemical calculations has been used.

## 3. RESULTS AND DISCUSSION

### 3.1. WEIGHT LOSS MEASUREMENTS

Fig. (1): represents the weight loss-time curves in the absence and presence of different concentrations of compound (1). Similar curves were obtained for other inhibitors (not shown). Table (2) collects the values inhibition efficiency obtained from weight loss measurements in 1 M H<sub>3</sub>PO<sub>4</sub> at 25 ± 0.1 °C. The results of this Table show that the presence of in-

Inhibitors reduce the corrosion rate of mild steel in 1 M H<sub>3</sub>PO<sub>4</sub> and hence, increase the inhibition efficiency. The inhibition achieved by these compounds decreases in the following order:

**Compound (1) > Compound (2) > Compound (3)**

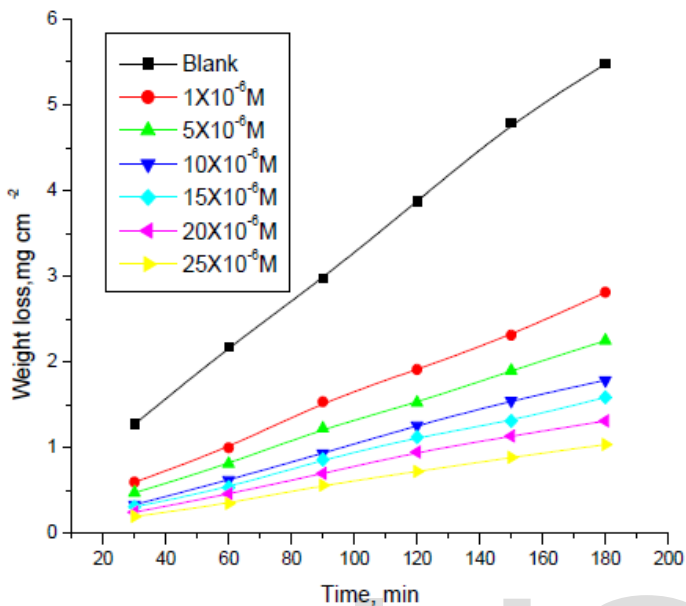


Fig.1. Weight Loss-Time Curves for the Dissolution of Mild Steel in the Absence and Presence of Different Concentrations of Inhibitor (1) in 1 M H<sub>3</sub>PO<sub>4</sub> at 25 ± 0.1 °C.

TABLE 2

INHIBITION EFFICIENCY OF ALL INHIBITORS AT DIFFERENT CONCENTRATIONS OF INHIBITORS AS DETERMINED FROM WEIGHT LOSS METHOD FOR MILD STEEL AT 25 ± 0.1 °C.

CONC., M	% IE		
	(1)	(2)	(3)
1X10 <sup>-6</sup>	49.0	33.2	27.8
5X10 <sup>-6</sup>	51.2	50.9	35.4
10X10 <sup>-6</sup>	70.3	59.3	51.7
15X10 <sup>-6</sup>	71.9	63.4	57.9
20X10 <sup>-6</sup>	78.4	67.9	64.1
25X10 <sup>-6</sup>	82.5	71.5	66.3

### 3.1.1. Adsorption Isotherm

Azole derivatives inhibit corrosion of mild steel by adsorbing onto the metal surface in acid solution. Basic information on the interaction between the inhibitor and the metal can be provided by the adsorption isotherm. The values of surface coverage ( $\theta$ ) corresponding to different concentrations of the inhibitor have been used to determine the adsorption isotherm. The variation of surface coverage ( $\theta$ ) determined by weight loss with the logarithm of the inhibitor (A) concentra-

tion with  $\log C$ , at different temperatures are represented in Fig. (2). Similar curves were obtained for other inhibitors (not shown). The linear relationships of  $\theta$  vs.  $\log C$  depicted in Fig. (2) with correlation coefficient nearly equal to 1.0 ( $R^2 > 0.989$ ) suggest that the adsorption of azole derivatives from 1 M H<sub>3</sub>PO<sub>4</sub> solution on mild steel obeys the Temkin adsorption isotherm. According to this isotherm the surface coverage is related to inhibitor concentration by:

$$K_{ads}C = \exp(-2a\theta) \quad (7)$$

Where "a" is the molecular interaction parameter and  $K_{ads}$  is the equilibrium constant of the adsorption process. The free energy of adsorption  $\Delta G^\circ_{ads}$  was calculated from the following equation [34]:

$$\Delta G^\circ_{ads} = -RT \ln(55.5K) \quad (8)$$

Where 55.5 is the concentration of water in solution in mol l<sup>-1</sup>, R is the universal gas constant and T is the absolute temperature. By applying the following the equation  $\Delta G^\circ_{ads} = \Delta H^\circ_{ads} - T \Delta S^\circ_{ads}$  and plot  $\Delta G^\circ_{ads}$  versus T linear relationships with slope equal ( $-\Delta S^\circ_{ads}$ ) and intercept of ( $\Delta H^\circ_{ads}$ ) were obtained. The data were collected in Table (3). From data in Table 3 we can conclude that:

- Negative sign of  $\Delta G^\circ_{ads}$  indicates that the adsorption of azole derivatives on mild steel surface is proceeding spontaneously [35, 36].
- Generally, values  $\Delta G^\circ_{ads}$  of up to  $-20 \text{ kJ mol}^{-1}$  are consistent with physisorption, while those around  $-40 \text{ kJ mol}^{-1}$  or higher are associated with chemisorptions as a result of the sharing or transfer of electrons from organic molecules to the metal surface to form a coordinate bond. From the obtained values of  $\Delta G^\circ_{ads}$  it was found the existence of comprehensive adsorption (physisorption and chemisorption) [37], that is to say, since the adsorption heat approached the general chemical reaction heat, the chemical adsorption occurs.
- Negative sign of  $\Delta H^\circ_{ads}$  indicates that the process of adsorption is exothermic [38].
- Positive sign of  $\Delta S^\circ_{ads}$  arises from substitutional process, which can be attributed to the increase in the solvent entropy. This lead to an increase in disorder due to the fact that more water molecules can desorbed from the metal surface by one inhibitor.

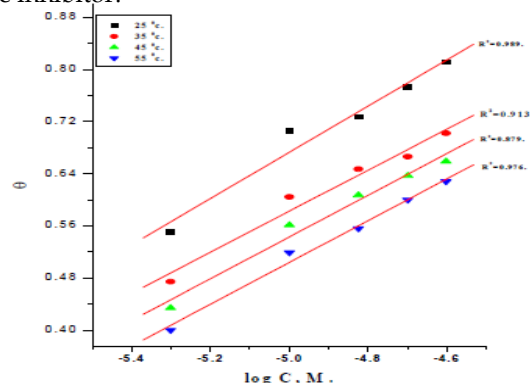


Fig. 2: Temkin Adsorption Isotherm for Mild Steel in 1 M H<sub>3</sub>PO<sub>4</sub> in the Presence of Different Concentrations of Inhibitor (1) at Different Temperatures.

TABLE 3

THERMODYNAMIC PARAMETERS FOR THE ADSORPTION OF AZOLE DERIVATIVES ON MILD STEEL SURFACE IN 1 M H<sub>3</sub>PO<sub>4</sub> AT DIFFERENT TEMPERATURES.

TEMP. °C	K <sub>ADS</sub> X10 <sup>-6</sup> M <sup>-1</sup>	-ΔG° <sub>ADS</sub> KJ MOL <sup>-1</sup>	-ΔH° <sub>ADS</sub> KJ MOL <sup>-1</sup>	ΔS° <sub>ADS</sub> J MOL <sup>-1</sup> K <sup>-1</sup>
(1)				
25	7.80	48.9	27.3	94.9
35	7.04	50.6		
45	4.90	51.3		
55	3.69	52.0		
(2)				
25	3.54	47.2	27.1	68.0
35	2.62	47.9		
45	2.17	48.8		
55	1.28	49.1		
(3)				
25	1.17	44.6	21.4	57.1
35	0.70	44.9		
45	0.56	45.7		
55	0.47	46.2		

3.1.2. EFFECT OF TEMPERATURE

The effect of temperature on both corrosion inhibition of mild steel in 1 M H<sub>3</sub>PO<sub>4</sub> solution in the absence and presence of different concentrations of inhibitors at different temperatures ranging from 25 to 55 °C was investigated. The apparent activation energies (E\*<sub>a</sub>) for the corrosion reaction of carbon steel in 1 M H<sub>3</sub>PO<sub>4</sub> solution in the absence and presence of different concentrations of benzothiazole derivatives were calculated from Arrhenius type equation [39]:

$$\text{Log } k_{\text{corr}} = \log A - E^*_a / (2.303RT) \quad (9)$$

Where A is the Arrhenius pre-exponential factor. A plot of log k<sub>corr</sub> versus 1/T gave straight lines as shown in Figure (3). The enthalpy of activation (ΔH\*) and the entropy of activation (ΔS\*) were obtained by applying the transition-state equation:

$$\log(k_{\text{corr}}/T) = [\log(R/Nh) + (\Delta S^*/2.303R) - (\Delta H^*/2.303RT)] \quad (10)$$

A plot of log (k<sub>corr</sub>/T) versus 1/T gave straight lines as shown in Figure (4). With a slope of (-ΔH\*/2.303R) and intercept of [log(R/Nh) + (ΔS\*/2.303R)] from which the values of ΔH\* and ΔS\* were calculated, respectively. All estimated thermodynamic-kinetic parameters were tabulated in Table (4). The obtained data in Table (4) can be interpreted as follows:

-The presence of inhibitors increases the activation energies of mild steel indicating strong adsorption of the inhibitor molecules on the metal surface and the presence of

these additives induces energy barrier for the corrosion reaction and this barrier increases with increasing the inhibitor concentrations.

-Higher activation energy means lower reaction rate and the opposite is true. The increase in activation energy with inhibitor concentration is often interpreted by physical adsorption with the formation of an adsorptive film of an electrostatic character.

-Values of ΔH\* are positive. This indicates that the corrosion process is an endothermic one.

-The entropy of activation (ΔS\*) in the absence and presence of inhibitor has negative values, this indicates that the activated complex in the rate determining step represents an association rather than dissociation, meaning that, a decrease in disordering takes place on going from reactants to the activated complex [40].

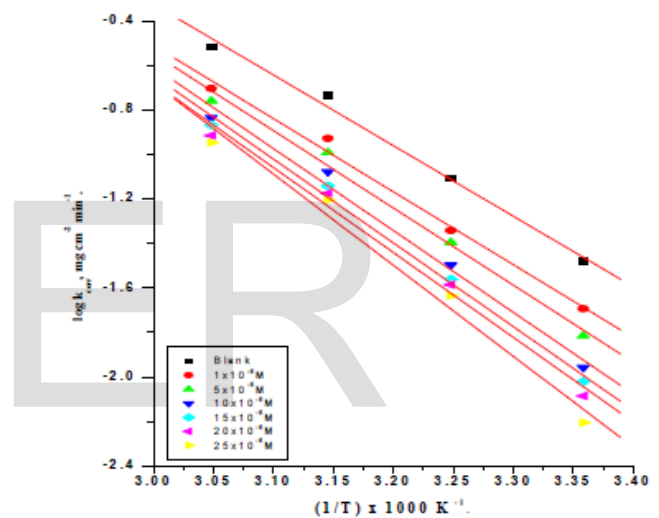


Fig. 3: Arrhenius Plots for Mild Steel Dissolution in 1 M H<sub>3</sub>PO<sub>4</sub> in the Absence and Presence of Different Concentrations of Inhibitor (1).

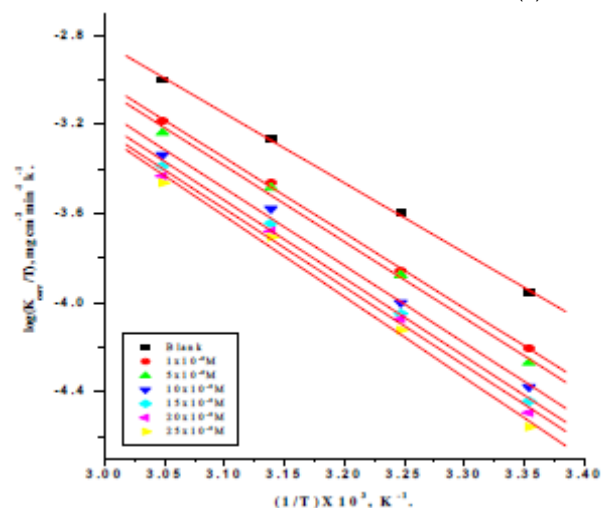


Fig.4: Transition State Plots for Mild Steel Dissolution in 1 M H<sub>3</sub>PO<sub>4</sub> in the Absence and Presence of Different Concentrations of Inhibitor (1).



TABLE 4

THERMODYNAMIC ACTIVATION PARAMETERS FOR THE DISSOLUTION OF MILD STEEL IN 1 M H<sub>3</sub>PO<sub>4</sub> IN THE ABSENCE AND PRESENCE OF DIFFERENT CONCENTRATIONS OF INVESTIGATED INHIBITORS.

INHIBITOR	CONC., M.	E <sub>A</sub> <sup>*</sup> KJ	ΔH <sup>*</sup> KJ	-ΔS <sup>*</sup> J MOL <sup>-1</sup>
BLANK	----	60.5	61.1	71.8
(1)	1 X 10 <sup>-6</sup>	62.7	65.0	67.1
	5 X 10 <sup>-6</sup>	66.8	65.7	59.7
	10 X 10 <sup>-6</sup>	70.9	66.8	58.8
	15 X 10 <sup>-6</sup>	71.8	66.9	58.0
	20 X 10 <sup>-6</sup>	73.0	67.9	57.8
	25 X 10 <sup>-6</sup>	77.9	69.8	50.9
(2)	1 X 10 <sup>-6</sup>	62.0	62.9	67.5
	5 X 10 <sup>-6</sup>	63.9	63.7	65.9
	10 X 10 <sup>-6</sup>	68.9	63.9	65.3
	15 X 10 <sup>-6</sup>	69.0	65.9	61.7
	20 X 10 <sup>-6</sup>	69.7	66.7	61.0
	25 X 10 <sup>-6</sup>	70.9	68.0	56.8
(3)	1 X 10 <sup>-6</sup>	61.4	61.6	68.7
	5 X 10 <sup>-6</sup>	62.9	62.7	68.0
	10 X 10 <sup>-6</sup>	66.6	63.7	65.9
	15 X 10 <sup>-6</sup>	66.5	65.0	61.6
	20 X 10 <sup>-6</sup>	67.4	65.2	61.2
	25 X 10 <sup>-6</sup>	68.9	66.1	60.2

### 3.2. Potentiodynamic Polarization Measurements

Figure (5) shows the potentiodynamic polarization curves for mild steel without and with different concentrations of compound (1) at 25 ± 0.1 °C. Similar curves were obtained for other compounds. The obtained electrochemical parameters; cathodic (β<sub>c</sub>) and anodic (β<sub>a</sub>) Tafel slopes, corrosion potential (E<sub>corr</sub>), and corrosion current density (i<sub>corr</sub>), were obtained and listed in Table. (5). Table. (5) shows that i<sub>corr</sub> decreases by adding theazole additives and by increasing their concentration. In addition, E<sub>corr</sub> does not change obviously. Also β<sub>a</sub> and β<sub>c</sub> do not change markedly, which indicates that the mechanism of the corrosion reaction of mild steel does not change. Figure. (5) clearly shows that both anodic and cathodic reactions are inhibited, which indicates that investigated compounds act as mixed-type inhibitors [41,42]. The inhibition achieved by these compounds decreases in the following order:

**Compound (1) > Compound (2) > Compound (3)**

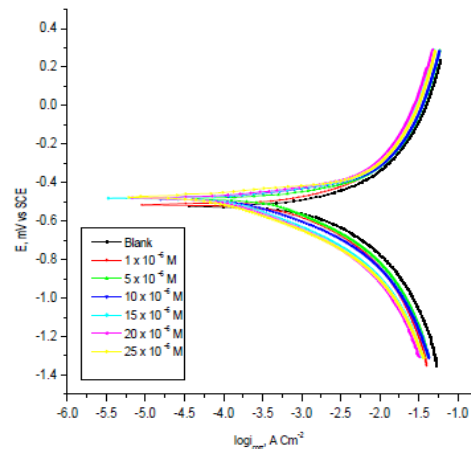


Fig. 5: Polarization Curves for the Dissolution of Mild Steel in 1 M H<sub>3</sub>PO<sub>4</sub> in the Absence and Presence of Different Concentrations of Compound (1) at 25 ± 0.1 °C.

TABLE 5

ELECTROCHEMICAL KINETIC PARAMETERS OBTAINED FROM POTENTIODYNAMIC POLARIZATION TECHNIQUE FOR THE CORROSION OF MILD STEEL IN 1 M H<sub>3</sub>PO<sub>4</sub> AT DIFFERENT CONCENTRATIONS OF INVESTIGATED INHIBITORS AT 25 ± 0.1 °C.

Inhibitor	Conc., M	-E <sub>corr</sub> , mV, vs SCE	i <sub>corr</sub> mA cm <sup>-2</sup>	β <sub>c</sub> mV dec <sup>-1</sup>	β <sub>a</sub> mV dec <sup>-1</sup>	θ	% IE
Blank	----	520	5.53	765	654	-----	-----
(1)	1 X 10 <sup>-6</sup>	511	2.57	641	543	0.535	53.5
	5 X 10 <sup>-6</sup>	486	2.40	611	497	0.566	56.6
	10 X 10 <sup>-6</sup>	477	1.09	469	396	0.802	80.2
	15 X 10 <sup>-6</sup>	466	0.65	439	364	0.882	88.2
	20 X 10 <sup>-6</sup>	456	0.53	418	352	0.904	90.4
	25 X 10 <sup>-6</sup>	477	0.34	377	311	0.938	93.8
(2)	1 X 10 <sup>-6</sup>	533	3.41	682	560	0.383	38.3
	5 X 10 <sup>-6</sup>	501	2.49	621	500	0.549	54.9
	10 X 10 <sup>-6</sup>	456	1.03	481	389	0.813	81.3
	15 X 10 <sup>-6</sup>	478	0.74	454	370	0.866	86.6
	20 X 10 <sup>-6</sup>	483	0.66	419	350	0.880	88.0
	25 X 10 <sup>-6</sup>	486	0.49	411	348	0.911	91.1
(3)	1 X 10 <sup>-6</sup>	519	3.83	712	587	0.307	30.7
	5 X 10 <sup>-6</sup>	521	3.44	680	564	0.377	37.7
	10 X 10 <sup>-6</sup>	521	2.65	644	532	0.520	52.0
	15 X 10 <sup>-6</sup>	513	1.80	560	466	0.674	64.5
	20 X 10 <sup>-6</sup>	517	1.45	525	422	0.737	73.7
	25 X 10 <sup>-6</sup>	519	1.26	479	442	0.772	77.2

### 3.3. Electrochemical Impedance Spectroscopy (EIS)

The corrosion of mild steel in 1 M H<sub>3</sub>PO<sub>4</sub> in the presence of the investigated compounds was investigated by EIS method at 25 ± 0.1 °C after 30 min immersion. Nyquist plots in the absence and presence of investigated compound (1) are presented in Fig. (6). Similar curves were obtained for other inhibitors. It is apparent that all Nyquist plots show a single capacitive loop, both in uninhibited and inhibited solutions. The impedance data of mild steel in 1 M H<sub>3</sub>PO<sub>4</sub> are analyzed in terms of an equivalent circuit model Fig. (7) which includes the solution resistance R<sub>s</sub> and the double layer capacitance C<sub>dl</sub> which is placed in parallel to the charge transfer resistance R<sub>ct</sub> [43] due to the charge transfer reaction. For the Nyquist plots it is

obvious that low frequency data are on the right side of the plot and higher frequency data are on the left. This is true for EIS data where impedance usually falls as frequency rises (this is not true for all circuits). The capacity of double layer ( $C_{dl}$ ) can be calculated from the following equation:

$$C_{dl} = \frac{1}{2\pi f_{max} R_{ct}} \quad (11)$$

Where  $f_{max}$  is maximum frequency. The parameters obtained from impedance measurements are given in Table (6). It can see from Table.(6) that the values of charge transfer resistance  $R_{ct}$  increase with inhibitor concentration [44]. In the case of impedance studies, % IE increases with inhibitor concentration in the presence of investigated inhibitors and the % IE of these investigated inhibitors is as follows:

**Compound (1) > Compound (3) > Compound (3)**

The impedance study confirms the inhibiting characters of these compounds obtained from potentiodynamic polarization and weight loss methods. It is also noted that the ( $C_{dl}$ ) values tend to decrease when the concentration of these compounds increases. This decrease in ( $C_{dl}$ ), which can result from a decrease in local dielectric constant and/or an increase in the thickness of the electrical double layer, suggests that these compounds molecules function by adsorption at the metal/solution interface [45]. The inhibiting effect of these compounds can be attributed to their parallel adsorption at the metal solution interface. The parallel adsorption is owing to the presence of one or more active center for adsorption.

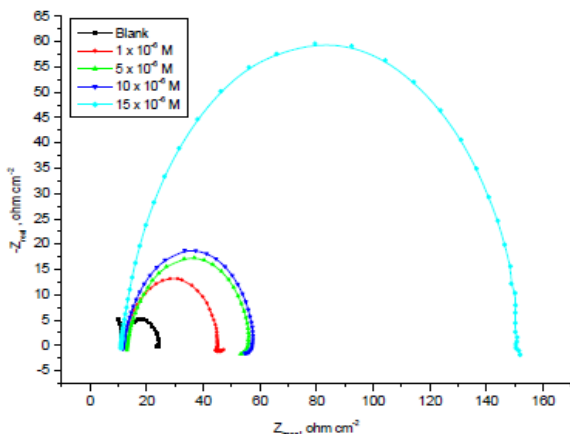


Fig. 6: Nyquist Plots for Mild Steel in 1 M  $H_3PO_4$  Solution in the Absence and Presence of Different Concentrations of Inhibitor (1) at  $25 \pm 0.1$  °C.

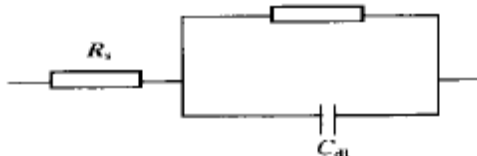


Fig. 7: Equivalent Circuit Model Used to Fit the Impedance Spectra

TABLE 6  
 ELECTROCHEMICAL KINETIC PARAMETERS OBTAINED FROM EIS TECHNIQUE FOR THE CORROSION MILD STEEL IN 1 M  $H_3PO_4$  AT DIFFERENT CONCENTRATIONS OF INVESTIGATED INHIBITORS AT AT  $25 \pm 0.1$  °C.

INHIBITOR	CONC., M	$C_{DL} \times 10^{-3}$ , MF $CM^{-2}$	$R_{ct}$ , $\Omega$ $CM^2$	$\Theta$	% IE
BLANK	-----	123.8	12.9	----	----
(1)	$1 \times 10^{-6}$	59.9	33.7	0.617	61.7
	$5 \times 10^{-6}$	46.9	43.0	0.700	70.0
	$10 \times 10^{-6}$	45.0	46.0	0.719	71.9
	$15 \times 10^{-6}$	29.9	146.5	0.911	91.1
(2)	$1 \times 10^{-6}$	55.5	29.2	0.558	55.8
	$5 \times 10^{-6}$	48.9	32.5	0.603	60.3
	$10 \times 10^{-6}$	55.9	35.5	0.636	63.6
	$15 \times 10^{-6}$	56.0	85.6	0.849	84.9
(3)	$1 \times 10^{-6}$	95.9	27.1	0.523	52.3
	$5 \times 10^{-6}$	82.0	28.8	0.552	55.2
	$10 \times 10^{-6}$	51.0	31.3	0.587	58.7
	$15 \times 10^{-6}$	46.3	34.2	0.622	62.2

**3.4. ELECTROCHEMICAL FREQUENCY MODULATION (EFM)**

Several authors proposed electrochemical frequency modulation (EFM) as a new electrochemical technique for online corrosion monitoring [46-49]. EFM is a rapid and nondestructive corrosion rate measurement technique that can directly give values of the corrosion current without prior knowledge of Tafel constants.

In corrosion research, it is known that the corrosion process is non-linear in nature, a potential distortion by one or more sine waves will generate responses at more frequencies than the frequencies of applied signal. Virtually no attention has been given to the intermodulation or electrochemical frequency modulation. However, EFM showed that this non-linear response contains enough information about the corroding system so that the corrosion current can be calculated directly. The great strength of the EFM is the causality factors which serve as an internal check on the validity of the EFM measurement. With the causality factors the experimental EFM data can be verified. Fig. (8) shows the current response contains not only the input frequencies, but also contains frequency components which are the sum, difference, and multiples of the two input frequencies.

- The larger peaks were used to calculate the corrosion current density ( $i_{corr}$ ), the Tafel slopes ( $\beta_a$  and  $\beta_c$ ) and the causality factors (CF-2 and CF-3). These electrochemical corrosion kinetic parameters at different concentrations of inhibitors in 1 M  $H_3PO_4$  at  $25 \text{ }^\circ\text{C} \pm 0.1 \text{ }^\circ\text{C}$ . were simultaneously determined and are listed in Table (7).
- The inhibition efficiency % IE increases by increasing the studied inhibitor concentrations. The causality factors CF-2 and CF-3 in Table (7) are close to their theoretical values of 2.0 and 3.0, respectively indicating that the measured data are of good quality.
- The calculated inhibition efficiency obtained from weight loss, Tafel polarization and EIS measurements are in good agreement with that obtained from EFM measurements.

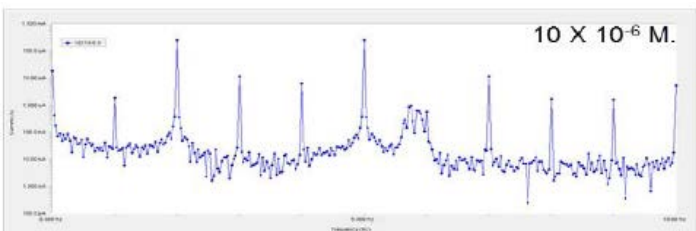
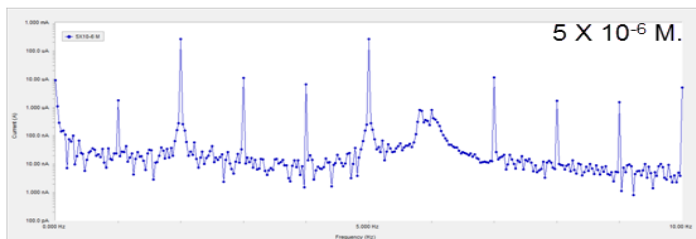
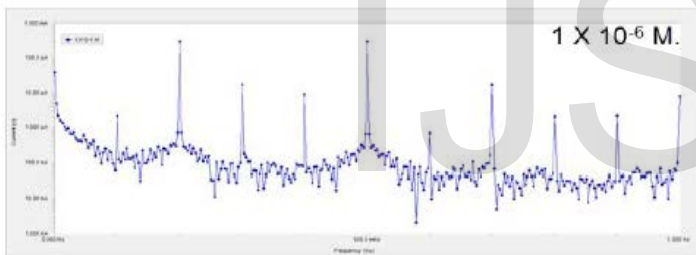
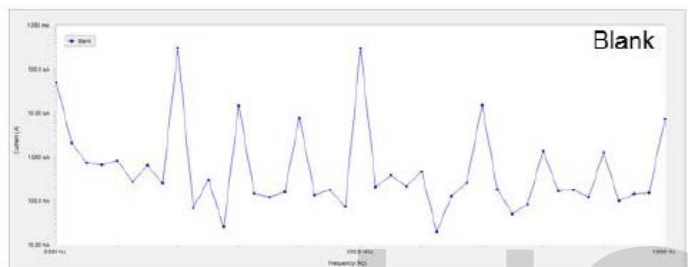


Fig. 8: EFM Spectra for Mild steel in 1 M  $H_3PO_4$  in the Absence and Presence of Different Concentrations of Compound (1) at  $25 \text{ }^\circ\text{C} \pm 0.1 \text{ }^\circ\text{C}$ .

TABLE 7

ELECTROCHEMICAL KINETIC PARAMETERS OBTAINED FROM EFM TECHNIQUE FOR MILD STEEL IN 1 M  $H_3PO_4$  IN THE ABSENCE AND PRESENCE OF DIFFERENT CONCENTRATIONS OF INVESTIGATED INHIBITORS

Inhibitor	Conc., M	$i_{corr}$ , $\mu\text{A cm}^{-2}$	$\beta_a$ , $\text{mV dec}^{-1}$	$\beta_c$ , $\text{mV dec}^{-1}$	CF-2	CF-3	% IE
Blank	---	949.0	153	296	1.99	3.05	-----
(1)	$1 \times 10^{-6}$	789.9	141	260	1.93	2.94	16.7
	$5 \times 10^{-6}$	589.0	190	195	1.97	3.03	37.9
	$10 \times 10^{-6}$	263.0	130	129	1.94	2.69	72.2
	$15 \times 10^{-6}$	236.5	122	130	1.96	2.92	75.0
(2)	$1 \times 10^{-6}$	800.0	149	232	1.98	2.90	15.7
	$5 \times 10^{-6}$	696.8	141	209	1.96	3.03	26.5
	$10 \times 10^{-6}$	591.1	133	221	1.91	3.20	37.7
	$15 \times 10^{-6}$	272.9	196	199	2.03	3.03	71.2
(3)	$1 \times 10^{-6}$	920.7	148	219	1.95	3.04	2.9
	$5 \times 10^{-6}$	811.1	151	219	1.94	2.73	14.5
	$10 \times 10^{-6}$	797.0	148	217	1.95	3.43	16.0
	$15 \times 10^{-6}$	617.9	131	201	1.94	2.88	34.8

### 3.5. Quantum chemical calculations

Theoretical calculations were performed for only the neutral forms, in order to give further insight into the experimental results. Values of quantum chemical indices such as energies of LUMO and HOMO ( $E_{HOMO}$  and  $E_{LUMO}$ ), and energy gap  $\Delta E$ , are calculated by semi-empirical AM1, MNDO and PM3 methods has been given in Table (8). The reactive ability of the inhibitor is related to  $E_{HOMO}$ ,  $E_{LUMO}$  [50]. Higher  $E_{HOMO}$  of the adsorbent leads to higher electron donating ability. Low  $E_{LUMO}$  indicates that the acceptor accepts electrons easily. The calculated quantum chemical indices ( $E_{HOMO}$ ,  $E_{LUMO}$ ,  $\mu$ ) of investigated compounds are shown in Table (8). The difference  $\Delta E = E_{LUMO} - E_{HOMO}$  is the energy required to move an electron from HOMO to LUMO. Low  $\Delta E$  facilitates adsorption of the molecule and thus will cause higher inhibition efficiency. The bond gap energy  $\Delta E$  increases from compound (1) to compound (3). This fact explains the decreasing inhibition efficiency in this order [Compound(1) > Compound(2) > Compound(3)], as shown in Table (8) and Figure (9) show the optimized structures of the three investigated compounds. So, the calculated energy gaps show reasonably good correlation with the efficiency of corrosion inhibition. Table (8) also indicates that compound (1) possesses the lowest total energy that

means that compound (1) adsorption occurs easily and is favored by the highest softness. The HOMO and LUMO electronic density distributions of these molecules were plotted in Figure (9). For the HOMO of the studied compounds that the benzene ring, N-atoms and O-atom have a large electron density. The data presented in Table (8) show that the calculated dipole moment decrease from [Compound(1) > Compound(2)> Compound(3)].

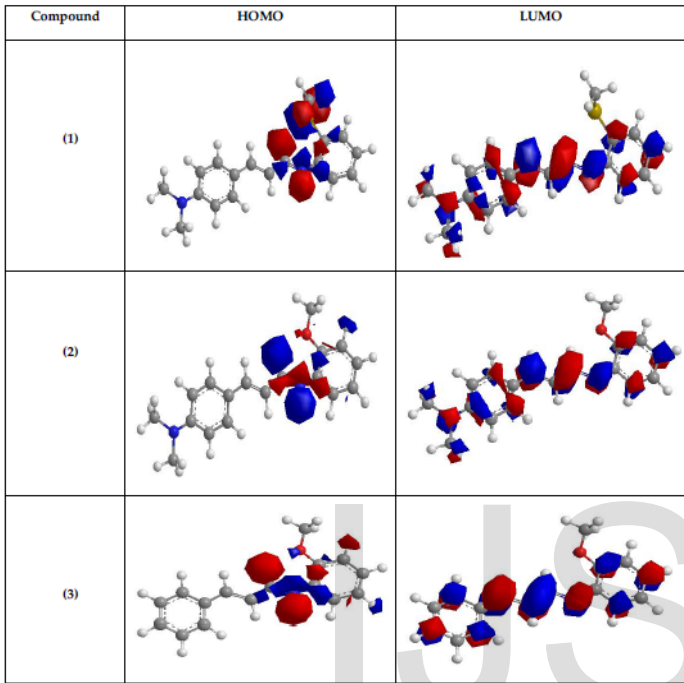


Fig. 9: Molecular Orbital Plots and Mulliken charges of Azole Compounds.

TABLE 8  
THE CALCULATED QUANTUM CHEMICAL PROPERTIES FOR  
AZOLE COMPOUNDS

	Compound (1)	Compound (2)	Compound (3)
-E <sub>HOMO</sub> (eV)	0.22714	0.27675	0.27672
-E <sub>LUMO</sub> (eV)	0.15956	0.19778	0.15559
ΔE (eV)	0.068	0.079	0.121
η (eV)	0.034	0.039	0.061
σ (eV <sup>-1</sup> )	29.595	25.326	16.511
-Pi (eV)	0.193	0.237	0.216
χ (eV)	0.193	0.237	0.216

#### 4- CHEMICAL STRUCTURE OF THE INHIBITORS AND CORROSION INHIBITION

Inhibition of the corrosion of mild steel in 1 M H<sub>3</sub>PO<sub>4</sub> solution by some azole compounds is determined by weight

loss, potentiodynamic anodic polarization measurements, Electrochemical Impedance Spectroscopy (EIS) and electrochemical frequency modulation method (EFM) Studies, it was found that the inhibition efficiency depends on concentration, nature of metal, the mode of adsorption of the inhibitors and surface conditions.

The observed corrosion data in presence of these inhibitors, namely:

- The decrease of corrosion rate and corrosion current with increase in concentration of the inhibitor.
- The linear variation of weight loss with time.
- The shift in Tafel lines to higher potential regions.
- The decrease in corrosion inhibition with increasing temperature indicates that desorption of the adsorbed inhibitor molecules takes place..
- The inhibition efficiency was shown to depend on the number of adsorption active centers in the molecule and their charge density.

It was concluded that the mode of adsorption depends on the affinity of the metal towards the π-electron clouds of the ring system. Metals such as Fe, which have a greater affinity towards aromatic moieties, were found to adsorb benzene rings in a flat orientation. The order of decreasing the percentage inhibition efficiency of the investigated inhibitors in the corrosive solution was as follow:

#### Compound(1) > Compound(2)> Compound(3)

Compound (1) exhibits excellent inhibition power due to; (i) its larger molecular size that may facilitate better surface coverage, and (ii) presence of sulphur atom which is more inhibition than oxygen atom.

Compound (2) comes after compound (1) in inhibition efficiency due to its lower molecular size than compound (1).

Compound (3) comes after compound (2) in inhibition efficiency, because it has lower molecular size than compound (2)

#### REFERENCES

- [1] Y. Jianguo, W. Lin, V. Otieno-Alego, D. P. Schweinsberg, Corros. Sci., 37 (1995).
- [2] E. E. Foad, El. Sherbini, Mater. Chem. Phys. 60 (1999) 286.
- [3] G. Lewis, Corros. Sci. 22 (1982) 579.
- [4] G. Schmitt, Br. Corros. J. 19 (1984) 165.
- [5] M. Bartos, N. Hackerman, J. Electrochem. Soc. 139 (1992) 3429.
- [6] S. L. Granese, Corrosion 44 (1988) 322.
- [7] F. Zucchi, G. Trabaneli, G. Brunoro, Corros. Sci. 33 (1992) 1135.
- [8] P. Chatterjee, M. K. Benerjee, K. P. Mukherjee, Indian J. Technol. 29 (1991) 191.
- [9] M. Elachouri, M. S. Hajji, S. Kertit, E. M. Essassi, M. Salem, R. Coudert, Corros. Sci. 37 (1995) 381.
- [10] B. Mernari, H. Elattari, M. Traisnel, F. Bentiss, M. Larenée, Corros. Sci. 40 (1998) 391.
- [11] F. Bentiss, M. Traisnel, N. Chaibi, B. Mernari, H. Vezin, M. Lagrenée, Corros. Sci. 44 (2002) 2271.
- [12] L. Elkadi, B. Mernari, M. Traisnel, F. Bentiss, M. Lagrenée, Corros. Sci. 42 (2000) 703.
- [13] A. Elkanouni, S. Kertit, A. Ben Bachir, Bull. Electrochem. 12 (1996) 517.
- [14] R. Walker, Corros. Sci. 31 (1975) 97.
- [15] S. Kertit, B. Hammouti, Appl. Surf. Sci. 93 (1996) 59.
- [16] M. El Azhar, B. Mernari, M. Traisnel, F. Bentiss, M. Lagrenée, Corros. Sci. 43 (2001) 2229
- [17] L. B. Tang, G.N. Mu, G.H. Liu, Corros. Sci. 45 (2003) 2251.



- [18] D. Q. Zhang, L.X. Gao, G.D. Zhou, J. Appl. Electrochem. 3 (2003) 361.
- [19] A. B. Tadros, B. A. Abdenaby, J. Electroanal. Chem. 246 (1988) 433.
- [20] L. Elkadi, B. Mernari, M. Traisnel, F. Bentiss, M. Lagrenée, Corros.Sci. 42 (2000) 703.
- [21] R. J. Chin, K. Nobe, J. Electrochem. Soc. 118 (1971) 545.
- [22] R. Agrawal, T.K.G. Nambodhiri, J. Appl. Electrochem. 22 (1972)383.
- [23] N. Eldakar, K. Nobe, Corrosion 32 (1976) 128.
- [24] F. Bentiss, M. Traisnel, M. Lagrenée, Corros. Sci. 42 (2000) 127.
- [25] W. Qafsaoui, H. Takenouti, Corros. Sci. 52(2010) 3667-3677.
- [26] M. Finsgar, I. Milosev, , Corros. Sci. 52(2010) 2737-2749.
- [27] M. L. Zheludkevich, K. A. Yasakau, S. K. Poznyak, M. G. S. Ferreira, Corros. Sci., 47 (2005) 3368-3383
- [28] F. Bentiss, M. Traisnel, L. Gengembre, M. Lagrenee, Appl. Surface Sci. 161(2000) 194-202.
- [29] I A. S. Fouda, A. S. Ellithy, Corros. Sci. 51(2009) 868-875.
- [30] H. L.Wang, R. B. Liu, J.Xin, Corros. Sci. 46 (2004) 2455-2466.
- [31] F. Bentiss, M. Lagrenee, M. Traisnel, J. C. Homez, Corros. Sci. 41(1999)789-803.
- [32] N. C. Desai and G. M. Kotadiya. Med Chem Res. 23 (2014) 4021-4033.
- [33] E. E. Oguzie . Mater. Letters, 59 (2005) 1076.
- [34] F. Bentiss, M. Traisnel, N. Chaibi, B. Mernari, H. Vezin, M. Lagrenée, Corros. Sci. 44 (2002) 2271.
- [35] A. A. El- Awady, B. Abd El-Nabey and S. G. Aziz, Electrochem. Soc. 139 (1992) 2149.
- [36] S. S. Abd El-Rehim, H. H. Hassan and M. A. Amin, Mater. Chem. Phys. 70 (2001) 64.
- [37] Li X. and Mu G, " Tween-40 , Appl. Surf. Sci., 252 (2005) 1254.
- [38] L. Tang, G. Murad and G. Liu, Corros. Sci. 45 (2003) 2251.
- [39] I. N. Putilova, S. A. Balzin and V. P. Barannik, Metallic Corrosion Inhibitors, Pergamomn Press , New York (1960) 31.
- [40] X. Li And L. Tang, Mater. Chem. Phys. 90 (2005) 286.
- [41] E.Stupnisek-Lisac, A.Gazivoda and M.Madzarac, J.Electrochim.Acta. 47 (2002) 4189.
- [42] G. N. Mu, X. H. L and Q. Quand J. Zhou, Corros. Sci. 48 (2006) 445.
- [43] I. Sekine, M. Sabongi, H. Hagiuda, T. Oshibe, M. Yuasa, T.Imahc, Y. Shibata, and T. Wake; J. Electrochem. Soc.; 139 (1992) 3167.
- [44] L. Larabi, O. Benali, S. M. Mekelleche and Y. Harek, Appl. Surf. Sci., 253 (2006) 1371.
- [45] M. Lagrenee, B. Mernari, B. Bouanis, M. Traisnel and F. Bentiss, Corros. Sci., 44 (2002) 573.
- [46] K. F. Khaled, Int. J. Electrochem. Sci., 3 (2005) 462.
- [47] K. F. Khaled, Electrochim. Acta, 53 (2008) 3484.
- [48] D. A. Jones, Principles and Prevention of Corrosion, second ed., Prentice Hall, Upper Saddle River, NJ, (1983).
- [49] R. W. Bosch, J. Hubrecht, W. F. Bogaerts, B. C. Syrett, Corrosion, 57 (2001) 60-70.
- [50] C. Lee, W. Yang and R. G. Parr., Phys. Rev. B, 37 (1988) 785.